Approximations for crossing two nearby spin resonances

V. H. Ranjbar

Brookhaven National Lab, Upton, New York 11973, USA

(Received 13 February 2014; published 7 January 2015)

Solutions to the Thomas-Bargmann-Michel-Telegdi spin equation for spin 1/2 particles have to date been confined to the single-resonance crossing. However, in reality, most cases of interest concern the overlapping of several resonances. While there have been several serious studies of this problem, a good analytical solution or even an approximation has eluded the community. We show that this system can be transformed into a Hill-like equation. In this representation, we show that, while the single-resonance crossing represents the solution to the parabolic cylinder equation, the overlapping case becomes a parametric type of resonance.

DOI: 10.1103/PhysRevSTAB.18.014001 PACS numbers: 29.20.D-, 29.27.Hj

I. INTRODUCTION

Two-level systems have been much studied in various branches of physics and have presented themselves early on in the development of quantum mechanics. In the accelerator physics community, similar problems emerge from the Thomas-BMT (Bargmann, Michel, and Telegdi) equation used to model the spin dynamics which particles undergo in a beam line. A well-developed theoretical apparatus exists to handle the various spin-depolarizing resonances. Essentially, it rests upon our understanding of solutions to the single-resonance model via the Froissart-Stora formula [1] for accelerating particles and harmonic oscillations for the stationary case.

However, in many cases, the presence of nearby spin resonances casts doubt upon the veracity of our understanding. So an approach to handle the interference of nearby spin resonances has been long sought after. Several efforts were made to understand the effect of nearby resonances. One approach based on classifying the proximity and strength of resonances was developed by Lee [2,3] and Tepikian [4] 18 years ago. However, this approach could not explain the case when the resonances nearly overlapped and the particle was accelerating. Later, in 2004, with some limited degree of success, Mane [5] developed an approximation based on the first-order Magnus expansion, and applied, *ad hoc*, a modified resonance strength to the Froissart-Stora formula. In this paper, we present an approach that casts the problem into a form permitting a clearer understanding of the underlying dynamics and admits a good perturbation approximation. Next, formulas are developed for the case when there is both zero and nonzero acceleration present. These new approximations might be of value for several current issues: For example, in the Alternating Gradient Synchrotron (AGS) and the Relativistic Heavy Ion Collider (RHIC), there are certain cases when imperfections and intrinsic resonances may be close enough and strong enough to warrant a treatment that considers the overlapping dynamics. In the RHIC lattice with the snakes off, this occurs at $G\gamma = 393 + \nu$, $411 - \nu$, where the intrinsic resonances are ≈ 0.4 at 10π mm mrad. At this strength, the intrinsic resonance can overlap either with its imperfection or with neighboring intrinsic resonances. It has been observed that this type of overlap can reduce the polarization transmission through the strong intrinsic resonances with snakes. For example, experience with a lattice designed to accommodate the phase advance necessary for the operation of the electron lens beam-beam compensation appears to show a reduced polarization transmission during the acceleration ramp. This new lattice has raised the strength of the neighboring resonances even while reducing the strong intrinsic resonance [6]. If taken individually, tracking and theory show that the two RHIC snakes should be enough to prevent depolarization at these resonance strengths. However, the overlapping mechanism appears to reduce the effectiveness of the snakes. In the AGS, the use of a strong partial snake might be modeled as a strong imperfection resonances, and, thus, the crossing of an intrinsic resonance may be considered as an overlapping intrinsic resonance with a strong imperfection resonance due to the partial snake [7]. This formalism might also be useful to analyze and reinterpret the phenomenon of spin echo, where the repeated crossings of given resonances can lead to spin recoherence [8]. Finally, it also could prove useful in extending the range of validity of the single-resonance analytical stroboscopic formula developed by Mane [9], since we will show that the single-resonance solution remains valid in the overlapping case, up to the onset of the parametric-resonance region. In the parametric-resonance region, the nonaccelerating formula derived here might be useful to develop a single turn spin map with snakes which can then provide solutions for the cases with rational tunes and perhaps irrational tunes following Mane's approach.

II. THOMAS-BMT EQUATION IN SPINOR FORM

The dynamics of the spin vector of a charged particle in the laboratory frame is described by the Thomas-BMT equation

$$\frac{d\vec{S}}{dt} = \frac{e}{\gamma m}\vec{S} \times ((1+G\gamma)\vec{B}_\perp + (1+G)\vec{B}_\parallel), \tag{1}$$

$\vec{S}$ is the spin vector of a particle in the rest frame, and $\vec{B}_\perp$ and $\vec{B}_\parallel$ are defined in the laboratory rest frame with respect to the particle's velocity. $G = \frac{g-2}{2}$ is the anomalous magnetic moment coefficient, and γmc^2 is the energy of the particle. Here we neglect the electric fields. We can transform this equation by expanding about a reference orbit described by the Frenet-Serret coordinate system shown in Fig. 1. Thus, we have

$$\frac{d\hat{x}}{ds} = \frac{\hat{s}}{\rho}, \qquad \frac{d\hat{s}}{ds} = -\frac{\hat{x}}{\rho}, \quad \text{and} \quad \frac{d\hat{z}}{ds} = 0, \tag{2}$$

where ρ is the local radius of curvature for the reference orbit. This is satisfactory for a trajectory in the plane (no vertical bends). Particle motion can be parameterized in this coordinate system as

$$\vec{r} = \vec{r}_o(s) + x\hat{x} + z\hat{z}. \tag{3}$$

Here, $\vec{r}_o(s)$ is the reference orbit, and $\hat{s} = d\vec{r}_o/ds$. The velocity becomes

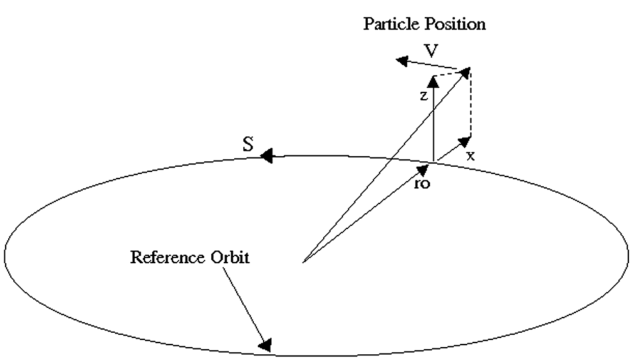

FIG. 1. The curvilinear coordinate system for a particle motion in a circular accelerator. $\hat{x}$, $\hat{s}$, and $\hat{z}$ are the transverse radial, the longitudinal, and the transverse vertical unit basis vectors, and $\vec{r}_0(s)$ is the reference orbit.

$$\begin{aligned}\vec{v} &= \frac{d\vec{r}}{dt}\\ &= \frac{ds}{dt}\left(x'\hat{x} + \left(1+\frac{x}{\rho}\right)\hat{s} + z'\hat{z}\right)\\ &\approx v(x'\hat{x} + \hat{s} + z'\hat{z}),\end{aligned} \tag{4}$$

$$\vec{v}' = v\left(\left(x'' - \frac{1}{\rho}\right)\hat{x} + \frac{x'}{\rho}\hat{s} + z''\hat{z}\right). \tag{5}$$

All primes $'$ represent derivatives with respect to s. The transverse magnetic field now can be expressed as

$$\begin{aligned}\vec{B}_\perp &= \frac{1}{v^2}(\vec{v}\times\vec{B})\times\vec{v}\\ &= B\rho\left(1-\frac{x}{\rho}\right)\left[\left(x''-\frac{1}{\rho}\right)\hat{z} + \frac{z'}{\rho}\hat{s} - z''\hat{x}\right],\end{aligned} \tag{6}$$

where we have employed $\frac{ds}{dt} \approx v(1-x/\rho)$ and $\vec{v}\times\vec{B} = \frac{\gamma mc}{e}\frac{d\vec{v}}{dt}$. We also note that $B_\perp\rho = \gamma mcv/e$ is the particle's magnetic rigidity. To the first order, $\vec{B}_\parallel$ is found to be

$$\vec{B}_\parallel \approx (B_s + B_z z')\hat{s}. \tag{7}$$

By using the dipole guiding field $B_z = -B_\perp\rho/\rho$, the B_s field can be derived from Maxwell's equations, obtaining

$$\frac{\partial B_s}{\partial z} = \frac{\partial B_z}{\partial s} = -(B\rho)\left(\frac{1}{\rho}\right)', \tag{8}$$

$$B_s = -B\rho z\left(\frac{1}{\rho}\right)'. \tag{9}$$

Neglecting higher-order terms,

$$\vec{B}_\parallel \approx -B\rho\left(\frac{z}{\rho}\right)'\hat{s}. \tag{10}$$

Then, by using $\frac{d}{dt} = \frac{v}{\rho+x}\frac{d}{d\theta}$, the Thomas-BMT equation becomes

$$\frac{d\vec{S}}{d\theta} = \vec{S}\times\vec{F}, \tag{11}$$

where $\vec{F} = F_1\hat{x} + F_2\hat{s} + F_3\hat{z}$, and the elements are

$$\begin{aligned}F_1 &= -\rho z''(1+G\gamma),\\ F_2 &= (1+G\gamma)z' - \rho(1+G)\left(\frac{z}{\rho}\right)',\\ F_3 &= -(1+G\gamma) + (1+G\gamma)\rho x''.\end{aligned} \tag{12}$$

By using $\frac{d\hat{x}}{d\theta} = \hat{s}$ and $\frac{d\hat{s}}{d\theta} = -\hat{x}$, Eq. (11) becomes

$$\frac{dS_1}{d\theta} = (1+F_3)S_2 - F_2 S_3,$$
$$\frac{dS_2}{d\theta} = -(1+F_3)S_1 + F_1 S_3,$$
$$\frac{dS_3}{d\theta} = F_2 S_1 - F_1 S_2. \qquad (13)$$

Expressed in the rotating frame, Eq. (11) then becomes

$$\frac{d\vec{S}}{d\theta} = \vec{n} \times \vec{S}, \qquad (14)$$

where $\vec{n} = -[F_1\hat{x} + F_2\hat{s} + (1+F_3)\hat{z}]$. Since we are concerned only with spin $1/2$ particles, we can employ the well-developed spinor formalism. By using the Pauli matrices

$$\sigma_x = \begin{pmatrix} 0 & 1 \\ 1 & 0 \end{pmatrix}, \qquad \sigma_s = \begin{pmatrix} 0 & -i \\ i & 0 \end{pmatrix},$$
$$\text{and} \quad \sigma_z = \begin{pmatrix} 1 & 0 \\ 0 & -1 \end{pmatrix}, \qquad (15)$$

the polarization can be given by

$$\vec{S} = \Psi^\dagger \vec{\sigma} \Psi. \qquad (16)$$

Then substituting Eq. (16) into the left side of Eq. (14) yields

$$\frac{d\vec{S}}{d\theta} = \frac{d\Psi^\dagger}{d\theta}\vec{\sigma}\Psi + \Psi^\dagger \vec{\sigma}\frac{d\Psi}{d\theta}. \qquad (17)$$

By using $[\vec{\sigma}\cdot\vec{n}, \vec{\sigma}] = 2i(\vec{n}\times\sigma)$, the right-hand side becomes

$$\vec{n}\times\vec{S} = -\frac{i}{2}(\Psi^\dagger\vec{\sigma})\vec{\sigma}\cdot\vec{n}\Psi + \frac{i}{2}\Psi^\dagger\vec{\sigma}\cdot n(\vec{\sigma}\Psi). \qquad (18)$$

Finally, equating both sides gives us

$$\frac{d\Psi}{d\theta} = -\frac{i}{2}\begin{pmatrix} f_3 & -\xi \\ \xi^* & -f_3 \end{pmatrix}\Psi, \qquad (19)$$

where $\xi(\theta) = F_1 - iF_2$ and $f_3 = (1+F_3)$ with

$$F_1 = -\rho z''(1+G\gamma),$$
$$F_2 = (1+G\gamma)z' - \rho(1+G)\left(\frac{z}{\rho}\right)',$$
$$F_3 = -(1+G\gamma) + (1+G\gamma)\rho x''. \qquad (20)$$

Here, θ is the orbital angle that remains constant outside the bends. Although the spinor function Ψ is similar in form to the quantum-mechanical-state function, in this case $\vec{S}$ is a classical vector. However, as in the former case, this two-component spinor is defined:

$$\Psi = \begin{pmatrix} u \\ d \end{pmatrix}. \qquad (21)$$

u and d are complex numbers representing the up and down components, respectively. The components of the spin vector become

$$S_1 = u^*d + ud^*,$$
$$S_2 = -i(u^*d - ud^*),$$
$$S_3 = |u|^2 - |d|^2. \qquad (22)$$

Because $H = (\vec{\sigma}\cdot\vec{n})$ is Hermitian,

$$|\vec{S}| = |u|^2 + |d|^2 = \Psi^\dagger\Psi, \qquad (23)$$

and the magnitude of the spin vector remains constant. We chose the normalization condition for the spinor function to be $\Psi^\dagger\Psi = 1$. Moving to the interaction frame by using the transformation

$$\Psi(\theta) = e^{-\frac{i}{2}\int_0^\theta f_3(t)dt\hat{\sigma}_z}\Psi_I(\theta),$$
$$\hat{\xi}(\theta) = \xi(\theta)e^{i\int_0^\theta f_3(t)dt} \qquad (24)$$

yields the following:

$$\frac{d\Psi_I^+}{d\theta} = \frac{i}{2}\hat{\xi}\Psi_I^-, \qquad \frac{d\Psi_I^-}{d\theta} = \frac{i}{2}\hat{\xi}^*\Psi_I^+. \qquad (25)$$

These equations can be cast into a standard second-order homogeneous linear differential equation with variable coefficients:

$$\frac{d^2\Psi_I^+}{d\theta^2} - \left(if_3(\theta) + \frac{\xi'(\theta)}{\xi(\theta)}\right)\frac{d\Psi_I^+}{d\theta} + \frac{\xi(\theta)\xi(\theta)^*}{4}\Psi_I^+ = 0. \qquad (26)$$

III. HILL-LIKE DIFFERENTIAL EQUATION

It is possible to eliminate the first-order derivative in Eq. (26) to obtain a Hill-like differential equation

$$\frac{d^2q}{d\theta^2} = \Omega^2(\theta)q \qquad (27)$$

by using the following definitions:

$$\beta(\theta) = -\left(if_3(\theta) + \frac{\xi'(\theta)}{\xi(\theta)}\right),$$
$$\Omega^2(\theta) = \frac{\beta'(\theta)}{2} + \frac{\beta(\theta)^2}{4} - \frac{\xi(\theta)\xi(\theta)^*}{4},$$
$$D(\theta) = \frac{1}{2}\int^\theta d\tau\beta(\tau), \qquad q(\theta) = e^{D(\theta)}\Psi_I^+(\theta). \qquad (28)$$

Evaluating $\Omega^2(\theta)$, we get

$$\Omega^2(\theta) = -\frac{if_3'}{2} - \frac{f_3^2}{4} + i\frac{f_3}{2}\left(\frac{\xi'(\theta)}{\xi(\theta)}\right) + \frac{3}{4}\left(\frac{\xi'(\theta)}{\xi(\theta)}\right)^2 - \frac{1}{2}\left(\frac{\xi''(\theta)}{\xi(\theta)}\right) - \frac{\xi(\theta)\xi(\theta)^*}{4}. \tag{29}$$

While formally this looks similar to Hill's equation, Ω^2 when undergoing acceleration is not periodic. Considering the form of Eq. (29), we see that $\Omega^2(\theta)$ will have oscillating terms from the transverse motion due to z. In fact, the standard approach is to expand $F_1 - iF_2$ into a Fourier series:

$$\xi(\theta) = F_1 - iF_2 = \sum_K \varepsilon_K e^{-iK\theta} \tag{30}$$

wherein the Fourier coefficient or resonance strength ε_K is given by the following:

$$\varepsilon_K = -\frac{1}{2\pi}\oint\left[(1+G\gamma)(\rho z'' + iz') - i\rho(1+G)\left(\frac{z}{\rho}\right)'\right]e^{iK\theta}d\theta. \tag{31}$$

Here, K is the resonance spin tune. Also, usually the $(1 + G\gamma)\rho x''$ term is ignored to first order. In the case when $G\gamma$ is constant, the equation reduces to a normal Hill equation with a constant piece defined by $G\gamma$ and an oscillating piece given by the Fourier expansion. In this case, we have parametric resonances whenever the constant- or polynomial- f_3 terms equal the frequency of the ξ terms. For a single resonance, the oscillating pieces coming from $\frac{\xi'(\theta)}{\xi(\theta)}$ and $\frac{\xi(\theta)\xi(\theta)^*}{4}$ cancel out each other, and the whole of $\Omega^2(\theta)$ is constant and becomes a simple harmonic oscillator. In the case $G\gamma(\theta)$ is not constant, but still we have only a single-resonance term in $\xi(\theta)$, then in $\Omega^2(\theta)$ all oscillating terms cancel each other as before, but we acquire a polynomial in θ. If the acceleration is linear, then it is a second-order polynomial solvable via Refs. [1,8]. In the case when there are both accelerating $G\gamma$ and multiple frequency terms in ξ, then $\Omega^2(\theta)$ has both polynomial and oscillating terms that make the solution much more challenging.

However, following Refs. [10,11], who considered a similar system with linear terms and multiple frequency terms, we can break up the Ω^2 into regions where the polynomial terms dominate and those where the parametric resonance dominates and then attempt a piecewise approximation that captures the important dynamics of this system.

Since the $\frac{1}{\xi(\theta)}$ term presents the most problems, we will expand this to obtain an adequate approximation. Considering only two resonances, one strong and the other weak, we expand to first order in the small parameter $\epsilon = a_2/a_1$, where a_1 is the absolute value of the stronger resonance ε_{K_1} and a_2 represents the weaker

$$\frac{1}{\xi(\theta)} = \frac{1}{a_1 e^{-i(K_1\theta+\phi_1)} + a_2 e^{-i(K_2\theta+\phi_2)}} \approx \frac{e^{i(K_1\theta+\phi_1)}}{a_1}(1 - (\epsilon e^{i\Delta\phi})e^{i\delta\theta}). \tag{32}$$

Here, $\phi_{1,2}$ are the phases of the ε_{K_1,K_2}, $\Delta\phi = \phi_1 - \phi_2$, and $\delta = K_1 - K_2$. Now, we can generate a new approximate $\beta(\theta)$ and $D(\theta)$:

$$\beta(\theta) \approx -(if_3(\theta) - iK_1 + i\delta\epsilon e^{i\delta\theta + i\Delta\phi}), \tag{33}$$

$$D(\theta) \approx \frac{1}{2}\left(\epsilon(1 - e^{i\delta\theta})e^{i\Delta\phi} - \frac{1}{2}i\theta(\alpha\theta + 2\kappa_0 - 2K_1)\right). \tag{34}$$

Here, we have assumed that $G\gamma$ is constantly ramping at the rate α, defining $f_3(\theta) = \kappa_0 + \alpha\theta$ with the initial $G\gamma_0 = \kappa_0$.

Now calculating Ω^2 we keep only the first-order terms in ϵ to get the following:

$$\begin{aligned}
\Omega^2(\theta) &\approx W_0^2 + C_1\theta + C_2\theta^2 + C_r(\theta)e^{i(\delta\theta+\Delta\phi)} + C_{-r}e^{-i(\delta\theta+\Delta\phi)},\\
W_0^2 &= -i\frac{\alpha}{2} - \frac{\kappa_0^2}{4} + \frac{K_1\kappa_0}{2} - \frac{K_1^2}{4} - \frac{a_1^2}{4},\\
C_1 &= \alpha\frac{K_1 - \kappa_0}{2}, \qquad C_2 = -\frac{\alpha^2}{4}, \qquad C_{-r} = -\epsilon\frac{a_1^2}{4},\\
C_r(\theta) &= \left(\left(-\frac{a_1^2}{4} + \frac{\delta^2}{2} + \frac{\delta(K_1 - \kappa_0)}{2}\right) - \frac{\alpha\delta}{2}\theta\right)\epsilon.
\end{aligned} \tag{35}$$

IV. OUTSIDE PARAMETRIC RESONANCE

It has been shown by Refs. [10,11] and others that, for a system which crosses a parametric resonance, a decent approximation can be achieved in a piecewise fashion. The oscillatory parts of the kernel contribute only inside the region of the so-called parametric-resonance tongue. This region is defined by using the following:

$$W_0^2 + C_1\theta + C_2\theta^2 \approx \delta^2/4 \pm |C_a|/2. \tag{36}$$

Here, C_a is the amplitude of the resonant oscillatory term. Outside the region of the parametric-resonant tongue, we can ignore the oscillatory pieces of Ω^2. The approximate Ω^2 for this region then becomes

$$\Omega_c^2(\theta) \approx W_0^2 + C_1\theta + C_2\theta^2. \tag{37}$$

For this Ω_c^2, solutions exist in the form of so-called parabolic cylinder functions $D_\nu(x)$. However, to provide easier contact with the standard derivation, this is really just the original solution to the single-resonance formula given in Refs. [1,8] [i.e., solving Eq. (26) with $\xi(\theta) = a_1 e^{-i(K_1\theta+\phi_1)}$].

This solution is valid up to the parametric-resonance-tongue region. For this particular case, the location of the dominant 2∶1 parametric resonance is $\theta = \theta_r$, which is found by solving Eq. (36) for θ setting $C_a = 0$:

$$\theta_{\pm r} = \mathrm{Re}\left[\frac{-C_1 \pm \sqrt{C_1^2 - C_2\delta^2 - 4C_2 W_0^2}}{2C_2}\right]. \quad (38)$$

So we see that there are two possible parametric-resonance regions represented by the two roots ($\theta_{\pm r}$). The boundaries for the parametric-resonance region are derived likewise by solving Eq. (36) for θ with now $C_a = |C_{+r}| + |C_{-r}|$, where $C_{+r} = C_r(\theta_r)$. So for the θ_{+r} root we have the following:

$$\theta_{+r\pm} \approx \mathrm{Re}\left[\frac{-C_1 + \sqrt{C_1^2 \pm 2C_2|C_a| - C_2\delta^2 - 4C_2 W_0^2}}{2C_2}\right], \quad (39)$$

where $+r\pm$ represents the two boundaries for the given parametric-resonance tongue. In Fig. 2, a plot of these boundaries is shown for one case. These two formulas for the location [Eq. (38)] and the boundaries for the parametric-resonance region [Eq. (39)] represent an important and potentially very useful result of this work. It demarks the locations in θ where the simpler single-resonance solution is valid.

One can also notice that Eq. (38) may have a nonzero imaginary part (which is why we take only the real part). This indicates that the parametric resonance is not on the real number line and we never actually cross that condition. However, the effects of the parametric resonance can still be observed provided $|C_a|$ is large enough as you can see in Fig. 3. This can be tested by seeing if $|C_a| \geq |2\Omega_c(\theta_{\pm r}) \pm \frac{\delta^2}{2}|$.

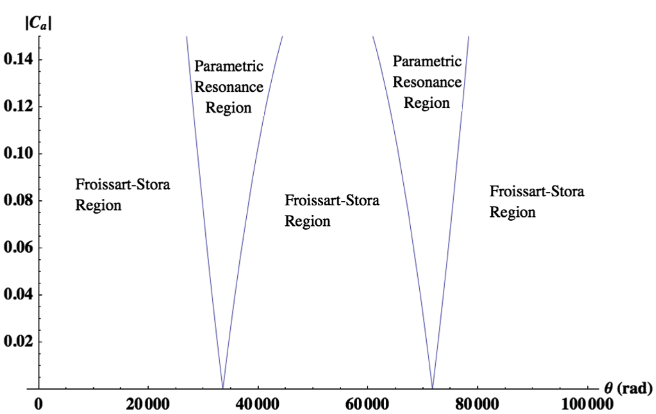

FIG. 2. $|C_a|$ versus orbital angle θ showing the two 2∶1 parametric-resonant-tongue regions. Here initial $G\gamma = \kappa_0 = 0.0$, $K_1 = 1.673$, $K_2 = 2.4$, and $\alpha = 3.18 \times 10^{-5}$.

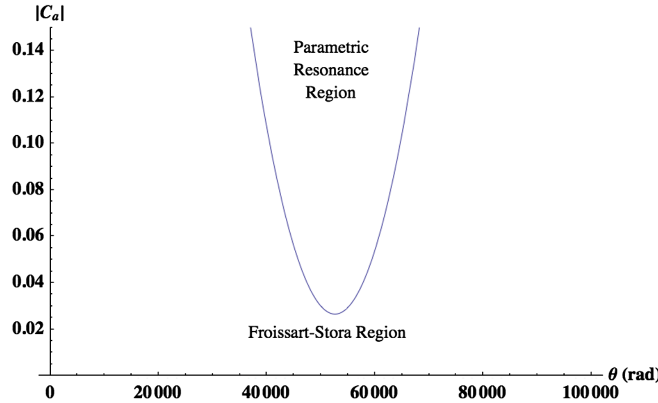

FIG. 3. $|C_a|$ versus orbital angle θ showing the two 2∶1 parametric-resonant-tongue region. Here initial $G\gamma = \kappa_0 = 0.0$, $K_1 = 1.673$, $K_2 = 2.0$, and $\alpha = 3.18 \times 10^{-5}$. Now the parametric-resonance region requires a minimum $|C_a| \geq 0.0265$ to cross.

V. INSIDE PARAMETRIC RESONANCE

Inside the parametric-resonant region, we must consider contributions to the solution from the oscillatory parts that are in resonance. So for our case, an approximate solution can be developed following Refs. [10,11], by using the multiscales method. We expand around the parametric resonance $\theta = \theta_r$ and rewrite $\Omega^2(\theta + \theta_r)$:

$$\Omega^2(\theta+\theta_r) \approx -\frac{\delta^2}{4} + \epsilon_1^2\mu\theta + \epsilon_1(se^{\pm(i\delta\theta+i\chi)} + \epsilon_2 e^{\mp(i\delta\theta+i\chi)}),$$
$$\epsilon_1 = |C_{\pm r}|, \qquad s = \mathrm{sgn}(C_{\pm r}), \qquad \sigma_1 = C_1 + 2C_2\theta_r,$$
$$\mu = \sigma_1/\epsilon_1^2, \qquad \epsilon_2 = C_{\mp r}/\epsilon_1, \qquad \chi = \delta\theta_r + \Delta\phi. \quad (40)$$

Here, we make several approximations. We drop both the $C_2\theta^2$ and $\epsilon^{\frac{\alpha\delta\theta}{2}}$ inside $C_r(\theta+\theta_r)$, since, during the resonance crossing (around θ_r), they are small relative to the other terms. We chose the $\pm$ equations, depending upon which terms $C_{\pm r}$ has the larger magnitude. Considering for now that C_{+r} is larger, we can follow Refs. [10,11]. By defining new coordinates $\eta = \epsilon_1\theta$ and $t = \theta$, our differential equation becomes (keeping only first-order ϵ_1 terms)

$$\frac{\partial^2 q}{\partial t^2} + 2\epsilon_1\frac{\partial^2 q}{\partial t\partial\eta} = \left(-\frac{\delta^2}{4} + \epsilon_1\mu\eta + \epsilon_1(se^{i\delta t+i\chi} + \epsilon_2 e^{-i\delta t-i\chi})\right)q. \quad (41)$$

Next, expanding $q = q_0 + \epsilon_1 q_1$ and collecting the zero and first-order terms in ϵ_1, we get

$$\frac{\partial^2 q_0}{\partial t^2} = -\frac{\delta^2}{4} q_0,$$
$$\frac{\partial^2 q_1}{\partial t^2} + 2\frac{\partial^2 q_0}{\partial t \partial \eta} = -\frac{\delta^2}{4} q_1 + q_0(\mu\eta + s e^{i\delta t + i\chi} + \epsilon_2 e^{-i\delta t - i\chi}). \tag{42}$$

The solution for the zeroth-order term is

$$q_0(\eta, t) = A(\eta) e^{i\delta t/2} + B(\eta) e^{-i\delta t/2}. \tag{43}$$

Canceling the secular terms in the q_1 equation leads us to a pair of coupled first-order equations for the A and B coefficients:

$$\frac{dB}{d\eta} = i\mu\eta/\delta B + i\epsilon_2/\delta e^{-i\chi} A, \tag{44}$$

$$\frac{dA}{d\eta} = -i\mu\eta/\delta A - is/\delta e^{i\chi} B. \tag{45}$$

This can be rewritten as a single second-order equation:

$$B'' = (i\mu/\delta + \epsilon_2 s/\delta^2 - \mu^2/\delta^2\eta^2) B, \tag{46}$$

whose two particular solutions are the parabolic cylinder functions

$$D_{-i\nu}\left(-(1-i)\sqrt{\frac{\sigma_1}{\delta}}\theta\right), \qquad D_{-1+i\nu}\left((1+i)\sqrt{\frac{\sigma_1}{\delta}}\theta\right), \tag{47}$$

with $\nu = \frac{\epsilon_2 s}{2\delta\mu}$. Using Eq. (44), we can develop a solution for $A(\eta)$. Thus, the q_0 approximation becomes the following:

$$\begin{aligned} q_0(\theta) &= B_1 q_0^{(1)}(\theta) + B_2 q_0^{(2)}(\theta), \\ q_0^{(1)}(\theta) &= \frac{e^{-\frac{i\delta\theta}{2}}}{\epsilon_1\epsilon_2}\left[(\epsilon_1\epsilon_2 - 2e^{i\chi + i\delta\theta}\sigma_1\theta) D_{-i\nu}\left(-(1-i)\sqrt{\frac{\sigma_1}{\delta}}\theta\right) + (-1-i)\sqrt{\delta}\sqrt{\sigma_1} e^{i\chi+i\delta\theta} D_{1-i\nu}\left(-(1-i)\sqrt{\frac{\sigma_1}{\delta}}\theta\right)\right], \\ q_0^{(2)}(\theta) &= \frac{e^{-\frac{i\delta\theta}{2}}}{\epsilon_1\epsilon_2}\left[(-1+i)\sqrt{\delta}\sqrt{\sigma_1} e^{i\chi+i\delta\theta} D_{i\nu}\left((1+i)\sqrt{\frac{\sigma_1}{\delta}}\theta\right) + \epsilon_1\epsilon_2 D_{-1+i\nu}\left((1+i)\sqrt{\frac{\sigma_1}{\delta}}\theta\right)\right]. \end{aligned} \tag{48}$$

It is also useful to give the values for $q_0^{(1,2)\prime}$:

$$\begin{aligned} q_0^{(1)\prime}(\theta) = -\frac{ie^{-\frac{1}{2}i\delta\theta}}{2\delta\epsilon_1\epsilon_2}\Bigg(&(\epsilon_1\epsilon_2(\delta^2 + 2\theta\sigma_1) + 2\sigma_1(-2\theta^2\sigma_1 + \delta(\delta\theta - 2i))e^{i(\delta\theta+\chi)}) D_{-i\nu}\left((-1+i)\theta\sqrt{\frac{\sigma_1}{\delta}}\right) \\ &+ (1+i)\sqrt{\delta}\Bigg(\left(-4\delta^{3/2}\theta\left(\frac{\sigma_1}{\delta}\right)^{3/2} e^{i(\delta\theta+\chi)} + \delta^2\sqrt{\sigma_1}e^{i(\delta\theta+\chi)} - 2\theta\sigma_1^{3/2}e^{i(\delta\theta+\chi)} + 2\sqrt{\delta}\epsilon_1\epsilon_2\sqrt{\frac{\sigma_1}{\delta}}\right) \\ &\times D_{1-i\nu}\left((-1+i)\theta\sqrt{\frac{\sigma_1}{\delta}}\right) + (-2-2i)\delta\sqrt{\sigma_1}\sqrt{\frac{\sigma_1}{\delta}}e^{i(\delta\theta+\chi)} D_{2-i\nu}\left((-1+i)\theta\sqrt{\frac{\sigma_1}{\delta}}\right)\Bigg)\Bigg), \end{aligned} \tag{49}$$

$$\begin{aligned} q_0^{(2)\prime}(\theta) = \frac{e^{-\frac{1}{2}i\delta\theta}}{2\delta\epsilon_1\epsilon_2}\Bigg(&-(1+i)\sqrt{\delta}\Bigg(\left(\delta^2\sqrt{\sigma_1}e^{i(\delta\theta+\chi)} + 2\theta\sigma_1^{3/2}e^{i(\delta\theta+\chi)} + 2\sqrt{\delta}\epsilon_1\epsilon_2\sqrt{\frac{\sigma_1}{\delta}}\right) D_{i\nu}\left((1+i)\theta\sqrt{\frac{\sigma_1}{\delta}}\right) \\ &+ (-2+2i)\delta\sqrt{\sigma_1}\sqrt{\frac{\sigma_1}{\delta}}e^{i(\delta\theta+\chi)} D_{i\nu+1}\left((1+i)\theta\sqrt{\frac{\sigma_1}{\delta}}\right)\Bigg) - i\epsilon_1\epsilon_2(\delta^2 - 2\theta\sigma_1) D_{i\nu-1}\left((1+i)\theta\sqrt{\frac{\sigma_1}{\delta}}\right)\Bigg). \end{aligned} \tag{50}$$

Solutions where the magnitude of C_{-r} is larger can be derived by permuting s with ϵ_2 in Eq. (48) and picking the corresponding $C_{\pm r}$ terms for $\epsilon_{1,2}$ in Eq. (40). With further consideration, expressions for $q_1(\theta)$ also can be developed, but they are large and the q_0 approximation usually suffices, since the important contributions of the order ϵ_1 terms come in via the $A(\eta)$ and $B(\eta)$ coefficients used in q_0. The $B_{1,2}$ coefficients can be found by using standard boundary-matching methods. One approach is to develop a matrix transport for these equations using the up and down spinors. This can be accomplished by using a matrix of the spin up and down solutions:

$$\vec{W}(\theta) = \begin{bmatrix} \psi_1^+(\theta) & \psi_2^+(\theta) \\ \psi_1^-(\theta) & \psi_2^-(\theta) \end{bmatrix} \tag{51}$$

with

$$\begin{aligned} \psi_{1,2}^+(\theta) &= q_0^{(1,2)}(\theta - \theta_r) e^{-D(\theta)}, \\ \psi_{1,2}^-(\theta) &= -2i\frac{\psi_{1,2}^{+\prime}(\theta)}{\hat{\xi}} \\ &= -2i\frac{e^{-D(\theta)}(q_0^{(1,2)\prime}(\theta) - \frac{1}{2}\beta(\theta) q_0^{(1,2)}(\theta))}{\hat{\xi}} \end{aligned} \tag{52}$$

for the parametric-resonance regions. Here we have used Eq. (25) to obtain the ψ^- solution. For the nonparametric region we have

$$\psi_1^+(\theta) = M\left(iq, \frac{1}{2}, \frac{i}{2}\alpha\theta^2\right),$$
$$\psi_2^+(\theta) = \frac{i}{2}a_1\theta e^{\frac{i}{2}\alpha\theta^2 - i\phi_1} M\left(1 - iq, \frac{3}{2}, -\frac{i}{2}\alpha\theta^2\right),$$
$$\psi_1^-(\theta) = -\psi_2^{+*}(\theta), \qquad \psi_2^+(\theta) = \psi_1^{+*}(\theta), \qquad q = \frac{a_1^2}{8\alpha}. \tag{53}$$

This is of course the Froissart-Stora derived solution [1]. $M(a,b,x)$ is the confluent hypergeometric function. Thus the spin transport map across each region from an arbitrary initial θ_i becomes

$$\vec{M}(\theta,\theta_i) = \vec{W}(\theta)\vec{W}^{-1}(\theta_i),$$
$$\Psi_I(\theta) = \vec{M}(\theta,\theta_i)\Psi_I(\theta_i). \tag{54}$$

So, for example, the transport matrix that can take one from a nonparametric-resonance region across a 2∶1 parametric resonance would look like

$$\vec{U}_{-r}(\theta,\theta_i) = \vec{M}_{fs}(\theta,\theta_{-r+})\vec{M}_{-r}(\theta_{-r+},\theta_{-r-})\vec{M}_{fs}(\theta_{-r-},\theta_i). \tag{55}$$

Here fs (Froissart-Stora) denotes the nonparametric-resonance region and $-r$ the θ_{-r} parametric-resonance region. In many cases, one crosses two parametric-resonance regions given by the two roots of Eq. (38) $\theta_{\pm r}$. Thus the total transport across the two regions becomes

$$\overrightarrow{UT}(\theta,\theta_i) = \vec{U}_{+r}(\theta,\theta_{+r-})\vec{U}_{-r}(\theta_{-r-},\theta_i),$$
$$\begin{pmatrix}\Psi(\theta)^+\\ \Psi(\theta)^-\end{pmatrix} = \overrightarrow{UT}(\theta,\theta_i)\begin{pmatrix}\Psi(\theta_i)^+\\ \Psi(\theta_i)^-\end{pmatrix}, \tag{56}$$

$$S_y(\theta) = 2|\Psi^+(\theta)|^2 - 1. \tag{57}$$

We have assumed that $\theta_{+r} > \theta_{-r}$ and that $\theta_{\pm r+} > \theta_{\pm r-}$. Depending on the values, this may or may not be true, and the matrices should naturally be adjusted according to their order in θ.

The transport matrices $\vec{M}_{fs}$ outside the parametric-resonance tongue are unitary; however, inside the parametric-resonance-tongue region, the perturbed solutions are not unitary. We can trivially enforce unitarity on the final result at any point by normalizing the up and down solutions (i.e., $\Psi_N^+ = \frac{\Psi_I^+}{\sqrt{|\Psi_I^+|^2+|\Psi_I^-|^2}}$). As will become evident in the section on error analysis, this does not appear to significantly degrade the accuracy of the final approximation.

VI. NONACCELERATING SOLUTIONS

It is noteworthy that we also can derive the nonaccelerating case (when $\alpha = 0$), starting from Eq. (46) and letting $\mu = 0$, since $\alpha = 0$. To ensure this approximation works well off the parametric resonance (this is lost when $\alpha = 0$), we also expand in powers of ϵ_1 about the parametric resonance ($\delta^2/4 = W_0^2$) and introduce a deviation w_1 from the parametric resonance to obtain

$$W_0^2 = \frac{\delta^2}{4} + \epsilon_1 w_1,$$
$$w_1 = \frac{W_0^2 - \delta^2/4}{\epsilon_1}. \tag{58}$$

We can now develop a new $A(\eta)$ and $B(\eta)$:

$$A(\eta) = \frac{\delta}{\epsilon_2}(B_1 f_- e^{f_0\eta} + B_2 f_+ e^{-f_0\eta}),$$
$$B(\eta) = B_1 e^{f_0\eta} + B_2 e^{f_0\eta}, \tag{59}$$

$$f_0 = \sqrt{\frac{s\epsilon_2 - w_1^2}{\delta^2}}, \tag{60}$$

$$f_\pm = \left(\frac{w_1}{\delta} \pm i f_0\right)e^{i\Delta\phi}, \tag{61}$$

and then a new $q_0(\theta)$:

$$q_0(\theta) = B_1 q_0^{(1)}(\theta) + B_2 q_0^{(2)}(\theta),$$
$$q_0^{(1)}(\theta) = e^{f_0\epsilon_1\theta}\left(f_+\frac{\delta}{\epsilon_2}e^{i\delta\theta/2} + e^{-i\delta\theta/2}\right),$$
$$q_0^{(2)}(\theta) = e^{-f_0\epsilon_1\theta}\left(f_-\frac{\delta}{\epsilon_2}e^{i\delta\theta/2} + e^{-i\delta\theta/2}\right). \tag{62}$$

In this case, there is benefit in adding the $q_1(\theta)$ term to our approximation, as one's energy deviates from the parametric resonance. As well, the additional terms are not so cumbersome as in the accelerating case. To accomplish this requires solving for q_1 in the following equation:

$$\frac{\partial^2 q_1}{\partial t^2} + 2\frac{\partial^2 q_0}{\partial t\partial\eta} = -\frac{\delta^2}{4}q_1 - q_0 w_1 + (se^{i\delta t + i\chi} + \epsilon_2 e^{-i\delta t - i\chi})q_0. \tag{63}$$

Using Eq. (59) for A and B cancels the secular terms, so we are left with the following nonhomogeneous equation:

$$\frac{\partial^2 q_1}{\partial t^2} + \frac{\delta^2}{4} q_1 = sA(\eta) e^{i3\delta t/2 + i\Delta\phi} + B(\eta)\epsilon_2 e^{-i3\delta t/2 - i\Delta\phi}. \tag{64}$$

This can be solved to give the first-order contribution:

$$\begin{aligned} q_1(\theta) &= B_1 q_1^{(1)}(\theta) + B_2 q_1^{(2)}(\theta), \\ q_1^{(1)}(\theta) &= \frac{e^{f_0\epsilon_1\theta}}{2\delta^2}\left(e^{i\frac{3\delta\theta}{2} - i\Delta\phi}\epsilon_2 + e^{-i\frac{3\delta\theta}{2} + \Delta\phi}\frac{s\delta f_-}{\epsilon_2}\right), \\ q_1^{(2)}(\theta) &= \frac{e^{-f_0\epsilon_1\theta}}{2\delta^2}\left(e^{i\frac{3\delta\theta}{2} - i\Delta\phi}\epsilon_2 + e^{-i\frac{3\delta\theta}{2} + \Delta\phi}\frac{s\delta f_+}{\epsilon_2}\right). \end{aligned} \tag{65}$$

As before, to obtain the (+) or (−) solutions, we just permute ϵ_2 and s depending on if C_{+r} is larger or C_{-r}. It is also useful to find the analogues of Eqs. (38) and (39), the location of the parametric resonance and its boundaries in κ_0 or $G\gamma$ space:

$$\kappa_{\pm r} = \pm\sqrt{-a_1^2 + \delta^2} + K_1, \tag{66}$$

$$\kappa_{+r\pm} = \sqrt{-a_1^2 \pm 2|C_a| + \delta^2} + K_1. \tag{67}$$

Here again $\pm r$ for Eq. (66) represent the two parametric resonances and $+r\pm$ for Eq. (67) the two resonance-tongue boundaries for each parametric resonance. With these solutions and boundaries, we can now build the spin transport matrices for Eq. (51). Now our $\psi_{1,2}^{\pm}$ become

$$\begin{aligned} q^{(1,2)}(\theta) &= q_0^{(1,2)}(\theta) + \epsilon_1 q_1^{(1,2)}(\theta), \\ \psi_{1,2}^{+}(\theta) &= q^{(1,2)}(\theta) e^{-D(\theta)}, \\ \psi_{1,2}^{-}(\theta) &= -2i\frac{\psi_{1,2}^{+\prime}(\theta)}{\hat{\xi}} \\ &= -2i\frac{e^{-D(\theta)}(q^{(1,2)\prime}(\theta) - \frac{1}{2}\beta(\theta) q^{(1,2)}(\theta))}{\hat{\xi}}. \end{aligned} \tag{68}$$

We also again derive the $q^{(1,2)\prime}$ values:

$$q^{(1)\prime}(\theta) = \frac{e^{-\frac{3i\delta\theta}{2} - i\Delta\phi + f_0\theta\epsilon_1}}{4\delta^2\epsilon_2}(2\delta^3 f_+ e^{i(2\delta\theta + \Delta\phi)}(2f_0\epsilon_1 + i\delta) + 2\delta^2\epsilon_2 e^{i(\delta\theta + \Delta\phi)}(2f_0\epsilon_1 - i\delta) + \epsilon_1\epsilon_2^2 e^{3i\delta\theta}(2f_0\epsilon_1 + 3i\delta) + \delta e^{(1+i)\Delta\phi} f_- s\epsilon_1(2f_0\epsilon_1 - 3i\delta)), \tag{69}$$

$$q^{(2)\prime}(\theta) = -\frac{ie^{-\frac{3i\delta\theta}{2} - i\Delta\phi - f_0\theta\epsilon_1}}{4\delta^2\epsilon_2}(-2\delta^3 f_- e^{i(2\delta\theta + \Delta\phi)}(\delta + 2if_0\epsilon_1) + 2\delta^2\epsilon_2 e^{i(\delta\theta + \Delta\phi)}(\delta - 2if_0\epsilon_1) - \epsilon_1\epsilon_2^2 e^{3i\delta\theta}(3\delta + 2if_0\epsilon_1) + \delta e^{(1+i)\Delta\phi} f_+ s\epsilon_1(3\delta - 2if_0\epsilon_1)). \tag{70}$$

As in the accelerating case, the transport matrices inside the parametric-resonance region are not unitary.

It is also worth pointing out that, for two special cases, an exact solution for q is possible. If the amplitude of either the positive or negative frequency dominates (i.e., $|\epsilon_2| \approx 0$), the other frequency can be ignored. For example, if $a_1^2 = 2\delta^2 + 2\delta(K_1 - \kappa_0)$, then the C_{+r} term is zero and the q differential equation becomes

$$\begin{aligned} q'' &= \left(W_0^2 - \frac{1}{4}a_1^2\epsilon e^{-i\delta\theta - i\Delta\phi}\right)q, \\ q^{(1)}(\theta) &= (-1)^{-\frac{iW_0}{\delta}}\Gamma\left(1 - \frac{2iW_0}{\delta}\right) I_{-\frac{2iW_0}{\delta}}\left(\frac{a_1\sqrt{\frac{e^{-i\Delta\phi - i\delta\theta}}{W_0^2}}W_0\sqrt{\epsilon}}{\delta}\right), \\ q^{(2)}(\theta) &= (-1)^{\frac{iW_0}{\delta}}\Gamma\left(\frac{2iW_0}{\delta} + 1\right) I_{\frac{2iW_0}{\delta}}\left(\frac{a_1\sqrt{\frac{e^{-i\Delta\phi - i\delta\theta}}{W_0^2}}W_0\sqrt{\epsilon}}{\delta}\right). \end{aligned} \tag{71}$$

Here $I_\nu(x)$ are modified Bessel functions of the first kind. Alternatively, if $|\epsilon_1| \approx 1$, which occurs when $|C_{+r}| = |C_{-r}|$, then the oscillating pieces become a single cosine or sine function, and again an exact analytical solution is possible via Mathieu functions. For example, when $\delta = 0$ or when $\delta = \kappa_0 - K_1$, we get

$$\begin{aligned} q'' &= \left(W_0^2 - \frac{1}{2}a_1^2\epsilon\cos(\delta\theta + \Delta\phi)\right)q, \\ q^{(1)}(\theta) &= \mathrm{MathieuC}\left[-\frac{4W_0^2}{\delta^2}, -\frac{a_1^2\epsilon}{\delta^2}, \frac{1}{2}(\delta\theta + \Delta\phi)\right], \\ q^{(2)}(\theta) &= \mathrm{MathieuS}\left[-\frac{4W_0^2}{\delta^2}, -\frac{a_1^2\epsilon}{\delta^2}, \frac{1}{2}(\delta\theta + \Delta\phi)\right]. \end{aligned} \tag{72}$$

VII. ERROR ANALYSIS

We compared 356 points, scanning the parameters between $\delta = 1$ to 0.001 from $a_1 = 0.0005$–1.0 and $a_2 = 0.0001$–0.1 at $\alpha = 3.18 \times 10^{-5}$ for $\Delta\phi = 0, \pi, \pi/2$ (see Fig. 4). For this sample, we kept the ratio of the dropped terms $\epsilon\frac{\alpha\delta\theta}{2} + C_2\theta^2$ to the remaining terms in Eq. (40) < 1 (this implies limits on δ, since C_{+r} and σ_1 have dependence

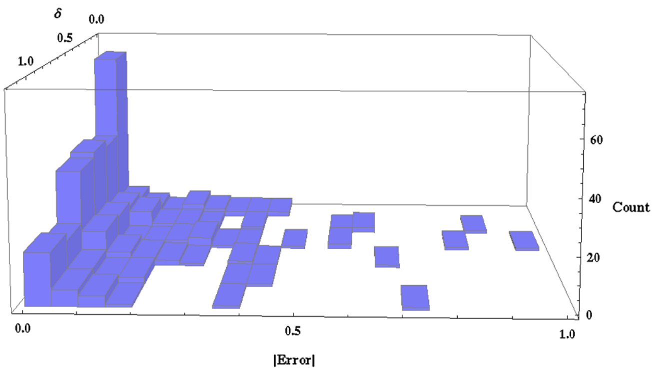

FIG. 4. A 3D histogram of δ and the absolute difference (|Error|) between approximation and numerically calculated values for the average final S_y (final 1000 rad) after crossing K_1 and K_2 (100 000 rad in orbital angle). This represents 356 parameters spanning $\delta = 1 - 0.001$, $a_1 = 0.0005$–1.0, and $a_2 = 0.0001$–0.1 at $\alpha = 3.18 \times 10^{-5}$ for $\Delta\phi = 0, \pi, \pi/2$.

on δ). When we compared our approximate results against direct numerical integration, as well as to the product of the Froissart-Stora formula applied to a_1 and a_2, we found that, when the absolute difference between the numerical and Froissart-Stora formula was $\geq 30\%$, our approximation provided a better result. This correlated with the region of "nearly and overlapping resonance" defined in Ref. [12] as $|\delta| \geq a_1$, and $|\delta| \gg a_2$. In this region, the average error for our approximation was 11%, while for Froissart-Stora it was 150%. However, we found for some particular values the errors for our approximation were $> 30\%$. These could be corrected by modifying the boundaries of the parametric-resonance region by ≈100 rad. We think that they represent the limits of our current approximation for the boundaries of the parametric-resonance region. Above $a_1 = 0.5$ and $a_2 = 0.1$, we also began to see the effects of the higher-order 1∶1 parametric resonances associated with $\Omega_c = \delta^2$. In this paper, we do not consider these parametric resonances. As exemplified in Fig. 5, our

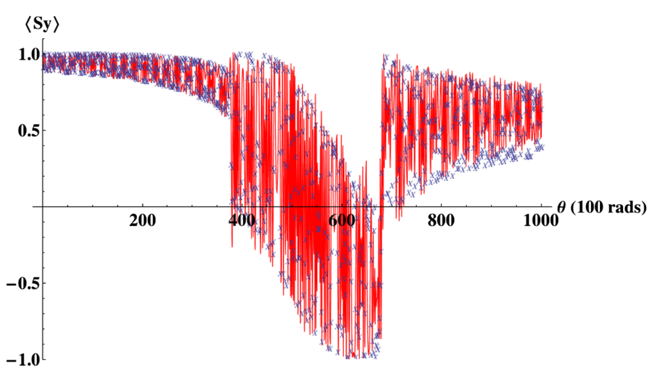

FIG. 5. S_y versus orbital angle θ with initial $G\gamma = \kappa_0 = 0.0$, $K_1 = 1.673$, $K_2 = 2.3$, $a_1 = 0.4$, $a_2 = 0.02$, $\Delta\phi = 0$, and $\alpha = 3.18 \times 10^{-5}$. The red trace is direct numerical integration; blue cross is piecewise approximation. One example is taken from scans shown in Fig. 4.

approximation also demonstrates an excellent qualitative agreement. At $\theta = 37426$ rad the first 2∶1 parametric resonance is apparent, and at $\theta = 67793$ rad the second is seen. We observed similar results for α at an order of magnitude slower (see Fig. 6). We have observed the range

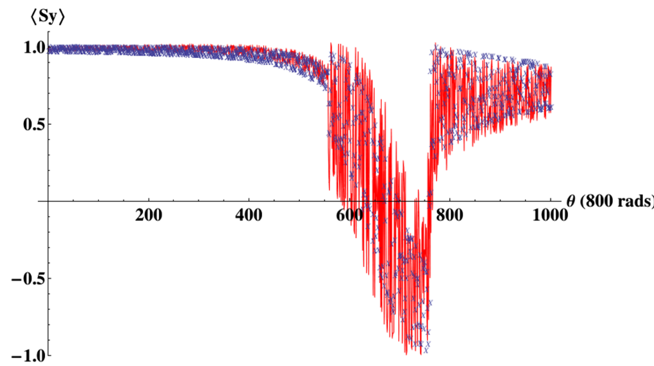

FIG. 6. S_y versus θ with initial $G\gamma = \kappa_0 = 0.0$, $K_1 = 1.673$, $K_2 = 2.0$, $a_1 = 0.2$, $a_2 = 0.005$, $\Delta\phi = 0$, and $\alpha = 3.18 \times 10^{-6}$. The red trace is direct numerical integration; blue cross is piecewise approximation.

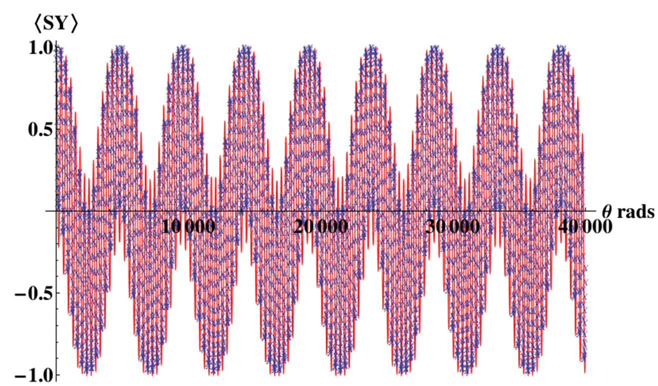

FIG. 7. Nonaccelerating case on parametric resonance. S_y versus θ with $\kappa_0 = 2.15583$ (on parametric resonance), $K_1 = 1.673$, $K_2 = 2.3$, $a_1 = 0.4$, $a_2 = 0.02$, and $\Delta\phi = 0$. The red trace is a direct numerical integration, while blue cross is calculated without the $\epsilon_1 q_1$ terms in Eq. (65).

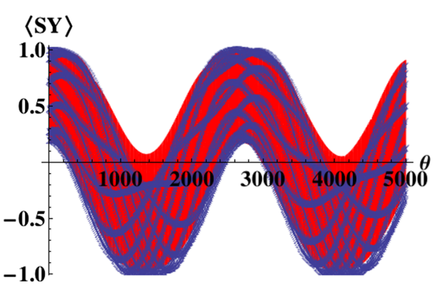

FIG. 8. Nonaccelerating case slightly off parametric resonance. S_y versus θ with $\kappa_0 = 1.19$, $K_1 = 1.673$, $K_2 = 2.3$, $a_1 = 0.4$, $a_2 = 0.02$, and $\Delta\phi = 0$. The red trace is a direct numerical integration, while blue cross is calculated by using Eq. (65).

of validity for α from 0 through 10^{-3}. It appears that we are limited in α only by our ability to resolve the boundaries of the parametric-resonance tongue. In Fig. 7, we compare the results of the nonaccelerating approximation to direct integration on a parametric resonance. For this case the zeroth-order approximation for the nonaccelerating case works well [Eq. (62)]. However, as we go off the parametric resonance while staying in the region of resonance tongues (see Fig. 8), the inclusion of the first-order terms appears to help.

VIII. CONCLUSION

We present a new formalism to handle the two-level problem which is common across many fields in physics (e.g., classical quantum mechanics, spintronic, and MRI). This approach transforms the problem into one of the passage through a parametric resonance that then is handled by using a multiscale technique to arrive at an analytic approximation. This is a significant improvement to Froissart-Stora in the overlap cases. Our work links the Thomas-BMT equation to the much-studied parametric-resonance tongues and, thus, offers a tool to easily predict the range of validity in θ [using Eqs. (38) and (39)] for the single-resonance approximation in a two-resonance system and also defines the location of the actual parametric resonance that in some cases can differ from K_2.

ACKNOWLEDGMENTS

I thank Mike Blaskiewicz and Mei Bai for their fruitful discussions and Mahshid Nirumand of Shiraz for her inspiration. This work was supported under Contract No. DE-AC02-98CH10886 with the U.S. Department of Energy and used National Energy Research Scientific Computing Center, which is supported by the Office of Science of the U.S. Department of Energy under Contract No. DE-AC02-05CH11231.

[1] M. Froissart and R. Stora, Nucl. Instrum. Methods **7**, 297 (1960).
[2] S. Y. Lee, Phys. Rev. E **47**, 3631 (1993).
[3] S. Y. Lee and M. Berglund, Phys. Rev. E **54**, 806 (1996).
[4] S. Tepikian *et al.*, *Part. Accel.* ***20****, 1 (1986)*.
[5] S. Mane, Nucl. Instrum. Methods Phys. Res., Sect. A **524**, 80 (2004).
[6] V. H. Ranjbar *et al.*, in *Proceedings of the 4th International Particle Accelerator Conference, IPAC-2013, Shanghai, China, 2013* (JACoW, Shanghai, China, 2013), p. 1544.
[7] H. Huang, L. A. Ahrens, M. Bai, K. Brown, E. D. Courant, C. Gardner, J. W. Glenn, F. Lin, A. U. Luccio, W. W. MacKay, M. Okamura, V. Ptitsyn, T. Roser, J. Takano, S. Tepikian, N. Tsoupas, A. Zelenski, and K. Zeno, Phys. Rev. Lett. **99**, 154801 (2007).
[8] A. Chao, Phys. Rev. ST Accel. Beams **8**, 104001 (2005).
[9] S. Mane, Nucl. Instrum. Methods Phys. Res., Sect. A **498**, 1 (2003).
[10] L. Ng, R. Rand, and M. O'Neil, J. Vib. Contr. **9**, 685 (2003).
[11] J. Bridge, R. Rand, and S. M. Sah, J. Vib. Contr. **15**, 1581 (2009).
[12] S. Y. Lee, *Spin Dynamics and Snakes in Synchrotrons* (World Scientific, Singapore, 1997).